Computational and Applied Mathematics (2020) 39:115
https://doi.org/10.1007/s40314-020-01141-7

The bivariate Müntz wavelets composite collocation method for solving space-time-fractional partial differential equations

Parisa Rahimkhani[1] · Yadollah Ordokhani[1]

Received: 23 April 2019 / Revised: 30 November 2019 / Accepted: 19 December 2019 /
Published online: 29 March 2020

Abstract
Herein, we consider an effective numerical scheme for numerical evaluation of three classes of space-time-fractional partial differential equations (FPDEs). We are going to solve these problems via composite collocation method. The procedure is based upon the bivariate Müntz–Legendre wavelets (MLWs). The bivariate Müntz–Legendre wavelets are constructed for first time. The bivariate MLWs operational matrix of fractional-order integral is constructed. The proposed scheme transforms FPDEs to the solution of a system of algebraic equations which these systems will be solved using the Newton's iterative scheme. Also, the error analysis of the suggested procedure is determined. To test the applicability and validity of our technique, we have solved three classes of FPDEs.

Keywords Bivariate Müntz–Legendre wavelets · Composite collocation method · Caputo derivative · Numerical technique

Mathematics Subject Classification 35R11 · 34K28 · 65M70

1 Introduction

In recent years, fractional equations appear in modeling of various real-life phenomena, for example dynamic viscoelasticity modeling (Larsson et al. 2015), hydrologic (Benson et al. 2013), economics (Baillie 1996), temperature and motor control (Bohannan 2008), solid mechanics (Rossikhin and Shitikova 1997), bioengineering (Magin 2004), medicine (Hall and Barrick 2008), porous media (He 1998), fluid-dynamic traffic model (He 1999), etc. Therefore, there is an increasing demand for numerical and analytical solutions of various types of fractional differential equations such as finite-difference/finite-element technique (Dehghan and Abbaszadeh 2018a, b, 2019), compact difference schemes (Hu and Zhang 2012), homotopy analysis method (Dehghan et al. 2010), homotopy perturbation method

Communicated by Vasily E. Tarasov.

✉ Yadollah Ordokhani
ordokhani@alzahra.ac.ir

1 Department of Mathematics, Faculty of Mathematical Sciences, Alzahra University, Tehran, Iran

(Abdulaziz et al. 2008), dual reciprocity boundary elements method (Dehghan and Safarpoor 2016), fifth-kind orthonormal Chebyshev polynomial method (Abd-Elhameed and Youssri 2018), B-spline functions (Lakestani et al. 2012), fractional-order Bernoulli function method (Rahimkhani et al. 2017), hybrid method (Mashayekhi and Razzaghi 2015), Legendre wavelet method (Heydari et al. 2014), fractional-order Lagrange polynomials (Sabermahani et al. 2018), fractional-order Bernoulli wavelets method (Rahimkhani et al. 2016), Müntz–Legendre wavelet method (Rahimkhani et al. 2018), etc.

Spectral schemes have received noticeable consideration for approximate solutions of various FPDEs, for example fractional diffusion equation (Lin and Xu 2007), fractional modified anomalous sub-diffusion equation (Dehghan et al. 2016), fractional cable equation (Lin et al. 2011), fractional Fokker–Planck equation (Zheng et al. 2015), FPDEs (Bhrawy and Zaky 2015), fractional advection–diffusion equations (Bhrawy and Baleanu 2013), etc.

In mathematical research, wavelets have been applied in different engineering fields for instance, signal analysis, image processing, edge extrapolation, optimal control problems, time–frequency analysis, fast algorithms, multiscale phenomena modeling, and pattern recognition (Chui 1997; Shamsi and Razzaghi 2005; Lakestani et al. 2006; Beylkin et al. 1991).

In recent years, diverse wavelets have been employed for numerical solution of several differential equations, for example Bernoulli wavelet (Rahimkhani et al. 2017), CAS wavelet (Saeedi et al. 2011), Chebyshev wavelet (Li 2010), second-kind Chebyshev wavelet (Zhu and Fan 2013), and Legendre wavelet (Rehman and Rahmat 2011; Heydari et al. 2013).

In this work, we present a computational scheme based on bivariate MLWs basis for solving three classes of FPDEs. First, bivariate MLWs are constructed. Then, we construct the bivariate MLWs' operation matrix of fractional integral. Finally, this operational is applied to convert the solution of the FPDEs to the solution of algebraic equations. Therefore, there are some questions to be answered:

- How to construct the Riemann–Liouville fractional integral operation matrix of bivariate MLWs.
- How to analyze FPDEs via fractional integration operational matrix of the bivariate MLWs.
- How to choose parameter of fractional-order (γ) of bivariate MLWs.
- How to select points of collocation methods.
- How long does CPU time of proposed method.

The current a paper is as follows:

In Sect. 2, we construct the bivariate MLWs and give some their properties. In Sect. 3, we derive the fractional-order integral operational matrix for bivariate MLWs. The problem is expressed in Sect. 4. In Sect. 5, a technique for numerical solution of three classes of FPDEs is presented. In Sect. 6, we give the convergence of approximate solution and the error of our scheme. Numerical findings are reported in Sect. 7. Also, Sect. 8 contains a conclusion.

2 Wavelets and bivariate MLWs

The bivariate MLWs are defined on $[0, 1) \times [0, 1)$ as:

$$\psi_{n,m,n',m'}(x,t)=\begin{cases}(2\lambda_m+1)^{\frac{1}{2}}(2\lambda_{m'}+1)^{\frac{1}{2}}2^{\frac{k+k'}{2}-1}L_m(2^{k-1}x-\hat{n})L_{m'}(2^{k'-1}t-\tilde{n}),\\ \qquad \frac{\hat{n}}{2^{k-1}}\le x<\frac{\hat{n}+1}{2^{k-1}},\ \frac{\tilde{n}}{2^{k'-1}}\le t<\frac{\tilde{n}+1}{2^{k'-1}},\\ 0, \qquad \text{otherwise},\end{cases} \tag{1}$$

where

$$\hat{n}=n-1,\tilde{n}=n'-1,\quad n=1,2,\ldots,2^{k-1};n'=1,2,\ldots,2^{k'-1},$$
$$m=0,1,2,\ldots,M-1;\quad m'=0,1,2,\ldots,M'-1;$$

and

$$\hat{m}=2^{k-1}M;\quad \tilde{m}=2^{k'-1}M'.$$

Here, $L_m(x)$ and $L_{m'}(t)$ are the Müntz–Legendre functions (MLFs) on [0, 1] as Rahimkhani et al. (2018):

$$L_m(x)=\sum_{s=0}^{m}c_{s,m}x^{\lambda_s},\quad c_{s,m}=\frac{\Pi_{j=0}^{m-1}(\lambda_s+\lambda_j+1)}{\Pi_{j=0,j\neq s}^{m}(\lambda_s-\lambda_j)},\quad (m\in N_0), \tag{2}$$

and

$$L_{m'}(t)=\sum_{s'=0}^{m'}c'_{s',m'}t^{\lambda_{s'}},\quad c'_{s',m'}=\frac{\Pi_{j=0}^{m'-1}(\lambda_{s'}+\lambda_j+1)}{\Pi_{j=0,j\neq s'}^{m'}(\lambda_{s'}-\lambda_j)},\quad (m'\in N_0). \tag{3}$$

These functions satisfy the following orthogonality condition: (Rahimkhani et al. 2018):

$$\int_0^1 L_n(x)L_m(x)dx=\frac{\delta_{n,m}}{(2\lambda_m+1)},\quad (m>n).$$

Also, the bivariate MLFs are defined on $[0,T_1)\times[0,T_2)$ as:

$$L_{m,n}(x,t)=\sum_{s'=0}^{m'}\sum_{s=0}^{m}c_{s,m}c'_{s',m'}\frac{x^{\lambda_s}t^{\lambda_{s'}}}{T_1^{\lambda_s}T_2^{\lambda_{s'}}}. \tag{4}$$

In this article, we consider $\lambda_k=k\gamma$, where γ is a real constant. Figures 1 and 2 demonstrate plots of 2D-MLWs for $\gamma=1$.

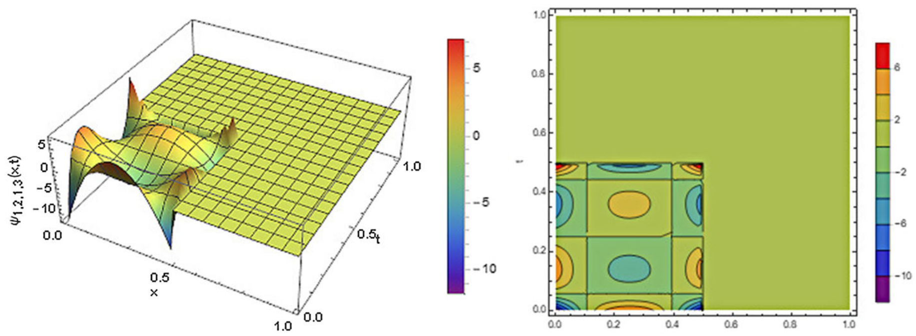

Fig. 1 Plot of 2D-MLWs and its contour with $n=n'=1$; $m=2$, $m'=3$ and $\gamma=1$

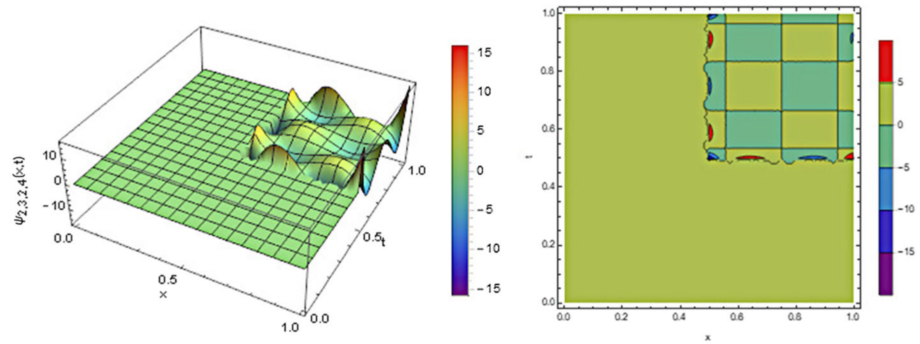

Fig. 2 Plot of 2D-MLWs and its contour with $n = n' = 2$; $m = 3, m' = 4$ and $\gamma = 1$

Remark 1 We consider order of Müntz–Legendre polynomials fits by paper (Esmaeili et al. 2011).

Let $f \in L^2\big([0, 1) \times [0, 1)\big)$ and the best approximation of f obtained using bivariate MLWs ($P^{k,k'}_{M,M'} f$), and then:

$$f(x,t) \simeq P^{k,k'}_{M,M'} f(x,t) = \sum_{n=1}^{2^{k-1}} \sum_{m=0}^{M-1} \sum_{n'=1}^{2^{k'-1}} \sum_{m'=0}^{M'-1} c_{n,m,n',m'} \psi_{n,m,n',m'}(x,t) \tag{5}$$

$$= \sum_{i=0}^{(\hat{m}\tilde{m})-1} c_i \psi_i(x,t) = C^T \Psi(x,t), \tag{6}$$

where

$$C = \left[c_0, c_1, c_2, \ldots, c_{(\hat{m}\tilde{m})-1}\right]^T, \tag{7}$$

and

$$\Psi(x,t) = \left[\psi_0(x,t), \psi_1(x,t), \psi_2(x,t), \ldots, \psi_{(\hat{m}\tilde{m})-1}(x,t)\right]^T. \tag{8}$$

3 Fractional integral operational matrix of bivariate MLWs

If $\Psi(x,t)$ is the vector in accordance with relation (8), then:

$${}^R_0 I^\alpha_x \Psi(x,t) = \Lambda(x,\alpha)\Psi(x,t) = (P_{\hat{m}\times\hat{m}}(x,\alpha) \otimes I_{\tilde{m}\times\tilde{m}})\Psi(x,t), \tag{9}$$

and

$${}^R_0 I^\alpha_t \Psi(x,t) = \Lambda'(t,\beta)\Psi(x,t) = (I_{\hat{m}\times\hat{m}} \otimes P'_{\tilde{m}\times\tilde{m}}(t,\beta))\Psi(x,t); \tag{10}$$

here:

- I is matrix of identity,
- $\Lambda(x,\alpha)$ and $\Lambda'(t,\beta)$ are $(\hat{m}\tilde{m}) \times (\hat{m}\tilde{m})$ the 2D-MLWs operational matrices of fractional-order integration,
- $P(x,\alpha)$ and $P'(t,\beta)$ are the 1D-MLWs operational matrices of fractional-order integration obtained on [0, 1) as Rahimkhani et al. (2018):

$$P(x,\alpha) = \zeta^{-1} F(x,\alpha)\zeta, \tag{11}$$

and

$$P'(t,\beta) = \zeta^{-1} F'(t,\beta)\zeta, \tag{12}$$

- ζ^{-1} is the convert matrix of the MLWs to the piecewise fractional-order Taylor functions (PFTFs),
- matrices $F(x,\alpha)$ and $F'(t,\alpha)$ are the PFTFs' operational matrices of fractional integration that these matrices are obtained in Rahimkhani et al. (2018).

4 Problem statement

In this study, we restrict ourselves on the following space-time FPDEs.

4.1 Problem a

The following FPDEs as:

$${}_0^C\mathcal{D}_x^{\alpha} u(x,t) = F\left(x, t, u(x,t), {}_0^C\mathcal{D}_x^{\beta} u(x,t), {}_0^C\mathcal{D}_t^{\nu} u(x,t)\right), \quad 0 \le x, t < 1, \tag{13}$$

with Dirichlet boundary conditions as:

$$u(x,0) = f_0(x), \quad u(0,t) = g_0(t), \quad u(1,t) = g_1(t), \tag{14}$$

where $1 < \alpha \le 2$, $0 < \beta, \nu \le 1$ and ${}_0^C\mathcal{D}^{\alpha}$ is Caputo fractional derivative.

4.2 Problem b

The FPDEs in Eq. (13) with boundary conditions as:

$$u(x,0) = f_0(x), \quad u(0,t) = h_1(t), \quad u_x(0,t) = h_2(t). \tag{15}$$

4.3 Problem c

The FPDEs with proportional delays as:

$${}_0^C\mathcal{D}_x^{\alpha} u(x,t) = F\left(x, t, u(a_0x, b_0t), {}_0^C\mathcal{D}_x^{\beta} u(a_1x, b_1t), {}_0^C\mathcal{D}_t^{\nu} u(a_2x, b_2t)\right), \quad 0 \le x, t < 1, \tag{16}$$

subject to the initial and boundary conditions in Eq. (14).

5 Description of the bivariate Müntz–Legendre wavelets composite collocation method

In this part, we introduced the 2D Müntz–Legendre wavelets composite collocation method. For this purpose, let $x_m (m = 0, 1, \ldots, M-1)$ and $t_{m'}$, $(m' = 0, 1, \ldots, M'-1)$ be zeros of the shifted Legendre polynomials $P_M(x)$ and $P_{M'}(t)$. Therefore, we define the composite collocation points as:

$$x_{nm} = \frac{1}{2^{k-1}}(x_m + n - 1), \quad n = 1, 2, \ldots, 2^{k-1}; m = 0, 1, \ldots, M-1, \tag{17}$$

$$t_{n'm'} = \frac{1}{2^{k'-1}}(t_{m'} + n' - 1), \quad n' = 1, 2, \ldots, 2^{k'-1}; m' = 0, 1, \ldots, M' - 1. \tag{18}$$

We use the bivariate MLWs' operational matrix of fractional-order integration, properties of Caputo fractional derivative, and the composite collocation scheme for solving problems (a), (b), and (c).

5.1 Problem a

For numerical solution of problem (a), we expand $\frac{\partial^{\alpha+\nu}u(x,t)}{\partial x^{\alpha}\partial t^{\nu}}$ by the bivariate MLWs as:

$$\frac{\partial^{\alpha+\nu}u(x,t)}{\partial x^{\alpha}\partial t^{\nu}} \simeq C^T \Psi(x,t). \tag{19}$$

Integrating of relation (19) of order ν with respect to t achieves:

$$\begin{aligned} {}_0^C\mathcal{D}_x^{\alpha} u(x,t) \simeq {}_0^C\mathcal{D}_x^{\alpha} P_{M,M'}^{k,k'} u(x,t) &= C^T \Lambda'(t,\nu)\Psi(x,t) + {}_0^C\mathcal{D}_x^{\alpha} u(x,t)\Big|_{t=0} \\ &= C^T \Lambda'(t,\nu)\Psi(x,t) + {}_0^C\mathcal{D}_x^{\alpha} f_0(x). \end{aligned} \tag{20}$$

Also, by fractional integration from Eq. (19) of order α with respect to x, we get:

$${}_0^C\mathcal{D}_t^{\nu} u(x,t) \simeq C^T \Lambda(x,\alpha)\Psi(x,t) + {}_0^C\mathcal{D}_t^{\nu} u(x,t)\Big|_{x=0} + x\frac{\partial}{\partial x}\left({}_0^C\mathcal{D}_t^{\nu} u(x,t)\right)\Big|_{x=0}. \tag{21}$$

We put $x = 1$ in Eq. (21), and using Eq. (14), we get:

$$\begin{aligned} {}_0^C\mathcal{D}_t^{\nu} u(x,t) \simeq {}_0^C\mathcal{D}_t^{\nu} P_{M,M'}^{k,k'} u(x,t) &= C^T \Lambda(x,\alpha)\Psi(x,t) \\ &\quad - xC^T \Lambda(1,\alpha)\Psi(1,t) + (1-x){}_0^C\mathcal{D}_t^{\nu} g_0(t) + x{}_0^C\mathcal{D}_t^{\nu} g_1(t). \end{aligned} \tag{22}$$

Integrating Eq. (20) of order α with respect to x yields:

$$u(x,t) \simeq C^T \Lambda'(t,\nu)\Lambda(x,\alpha)\Psi(x,t) + f_0(x) - f_0(0) - xf_0'(0) + g_0(t) + x\frac{\partial u(x,t)}{\partial x}\Big|_{x=0}. \tag{23}$$

We let $x = 1$ in Eq. (23), and considering Eq. (14), then Eq. (23) can be expressed as:

$$\begin{aligned} u(x,t) \simeq P_{M,M'}^{k,k'} u(x,t) &= C^T \Lambda'(t,\nu)\Lambda(x,\alpha)\Psi(x,t) \\ &\quad - xC^T \Lambda'(t,\nu)\Lambda(1,\alpha)\Psi(1,t) + \omega(x,t), \end{aligned} \tag{24}$$

where

$$\omega(x,t) = g_0(t) + f_0(x) - f_0(0) - xf_0'(0) + x\left(g_1(t) - g_0(t)\right) + x\left(-f_0(1) + f_0(0) + f_0'(0)\right).$$

By derivative of order β with respect to x from Eq. (24), we get:

$$\begin{aligned} {}_0^C\mathcal{D}_x^{\beta} u(x,t) \simeq {}_0^C\mathcal{D}_x^{\beta} P_{M,M'}^{k,k'} u(x,t) &= C^T \Lambda'(t,\nu)\Lambda(x,\alpha-\beta)\Psi(x,t) \\ &\quad - \frac{x^{1-\beta}}{\Gamma(2-\beta)} C^T \Lambda'(t,\nu)\Lambda(1,\alpha)\Psi(1,t) + {}_0^C\mathcal{D}_x^{\beta}\omega(x,t). \end{aligned} \tag{25}$$

By substituting above approximations into Eq. (13) and replacing $\simeq$ by $=$ and collocating this equation at the composite collocation points given into Eqs. (17) and (18), we achieve:

$${}_0^C\mathcal{D}_x^{\alpha} P_{M,M'}^{k,k'} u(x_{n,m}, t_{n',m'}) = F(x_{n,m}, t_{n',m'}, P_{M,M'}^{k,k'} u(x_{n,m}, t_{n',m'}),$$

$$
\begin{aligned}
&{}^{C}_{0}\mathcal{D}^{\beta}_{x} P^{k,k'}_{M,M'} u(x_{n,m}, t_{n',m'}), {}^{C}_{0}\mathcal{D}^{\nu}_{t} P^{k,k'}_{M,M'} u(x_{n,m}, t_{n',m'})),\\
&n = 1, 2, \ldots, 2^{k-1}, \quad m = 0, 1, \ldots, M-1,\\
&n' = 1, 2, \ldots, 2^{k'-1}, \quad m' = 0, 1, \ldots, M'-1.
\end{aligned} \tag{26}
$$

Equation (26) gives $\hat{m} \times \tilde{m}$ equations, after solving this system by applying Newton's iterative scheme (Stoer and Bulirsch 2002), we get unknown vector C^T.

For example 1, when $k = k' = 2$, $M = M' = 2$ and $\gamma = 1$, we let: $c_i^{(0)} = 0, \quad , i = 0, \ldots, 15$.

Using Newton's iterative scheme, we get:

$$
\begin{aligned}
c_0^{(1)} &= c_0^{(2)} = \cdots = 0.210757,\\
c_1^{(1)} &= c_1^{(2)} = \cdots = 0.144816,\\
c_2^{(1)} &= c_2^{(2)} = \cdots = 1.38863,\\
c_3^{(1)} &= c_3^{(2)} = \cdots = 0.12982,\\
c_4^{(1)} &= c_4^{(2)} = \cdots = 0.101842,\\
c_5^{(1)} &= c_5^{(2)} = \cdots = 0.0710262,\\
c_6^{(1)} &= c_6^{(2)} = \cdots = 0.457712,\\
c_7^{(1)} &= c_7^{(2)} = \cdots = 0.035036,\\
c_8^{(1)} &= c_8^{(2)} = \cdots = 0.106264,\\
c_9^{(1)} &= c_9^{(2)} = \cdots = 0.0621804,\\
c_{10}^{(1)} &= c_{10}^{(2)} = \cdots = 0.216712,\\
c_{11}^{(1)} &= c_{11}^{(2)} = \cdots = 0.028955,\\
c_{12}^{(1)} &= c_{12}^{(2)} = \cdots = 0.0528427,\\
c_{13}^{(1)} &= c_{13}^{(2)} = \cdots = 0.0320725,\\
c_{14}^{(1)} &= c_{14}^{(2)} = \cdots = 0.157604,\\
c_{15}^{(1)} &= c_{15}^{(2)} = \cdots = 0.0320673.
\end{aligned}
$$

5.2 Problem b

For solving problem (b), we expand $\frac{\partial^3 u(x,t)}{\partial x^2 \partial t}$ by the bivariate MLWs as:

$$
\frac{\partial^3 u(x,t)}{\partial x^2 \partial t} \simeq C^T \Psi(x,t). \tag{27}
$$

Integrating with respect to x of Eq. (27) gives:

$$
\frac{\partial^2 u(x,t)}{\partial x \partial t} \simeq C^T \Lambda(x,1)\Psi(x,t) + \left.\frac{\partial^2 u(x,t)}{\partial x \partial t}\right|_{x=0} = C^T \Lambda(x,1)\Psi(x,t) + h_2'(t). \tag{28}
$$

Also, integrating from Eq. (27) with respect to t:

$$
\frac{\partial^2 u(x,t)}{\partial x^2} \simeq C^T \Lambda'(t,1)\Psi(x,t) + \left.\frac{\partial^2 u(x,t)}{\partial x^2}\right|_{t=0} = C^T \Lambda'(t,1)\Psi(x,t) + f_0''(x). \tag{29}
$$

Integrating with respect to x of Eq. (28) gives:

$$\frac{\partial u(x,t)}{\partial t} \simeq C^T \Lambda^2(x,1)\Psi(x,t) + h_2'(t)x + \left.\frac{\partial u(x,t)}{\partial t}\right|_{x=0}$$
$$= C^T \Lambda^2(x,1)\Psi(x,t) + h_2'(t)x + h_1'(t), \tag{30}$$

and

$$u(x,t) \simeq C^T \Lambda^2(x,1)\Lambda'(t,1)\Psi(x,t) + \varpi(x,t), \tag{31}$$

where

$$\varpi(x,t) = x(h_2(t) - h_2(0)) + (h_1(t) - h_1(0)) + f_0(x).$$

For $1 < \alpha \leq 2$ by integrating from Eq. (29) with respect to x of order $2-\alpha$, we achieve:

$${}_0^C\mathcal{D}_x^{\alpha} u(x,t) = {}_0^R I_x^{2-\alpha}\left(\frac{\partial^2 u(x,t)}{\partial x^2}\right) \simeq C^T \Lambda'(t,1)\Lambda(x,2-\alpha)\Psi(x,t) + {}_0^R I_x^{2-\alpha}{}_0^C\mathcal{D}_x^2 f_0(x)$$
$$= C^T \Lambda'(t,1)\Lambda(x,2-\alpha)\Psi(x,t) + {}_0^C\mathcal{D}_x^{\alpha} f_0(x). \tag{32}$$

Also, for $0 < \nu \leq 1$ by integrating from Eq. (30) with respect to t of order $1-\nu$, we get:

$${}_0^C\mathcal{D}_t^{\nu} u(x,t) = {}_0^R I_t^{1-\nu}\left(\frac{\partial u(x,t)}{\partial t}\right) \simeq C^T \Lambda^2(x,1)\Lambda'(t,1-\nu)\Psi(x,t)$$
$$+x{}_0^R I_t^{1-\nu}{}_0^C\left(\frac{\partial h_2(t)}{\partial t}\right) + {}_0^R I_t^{1-\nu}{}_0^C\mathcal{D}_t\left(\frac{\partial h_1(t)}{\partial t}\right)$$
$$= C^T \Lambda^2(x,1)\Lambda'(t,1-\nu)\Psi(x,t) + x{}_0^C\mathcal{D}_t^{\nu} h_2(t) + {}_0^C\mathcal{D}_t^{\nu} h_1(t). \tag{33}$$

By derivative from Eq. (31) with respect to x of order β yields:

$${}_0^C\mathcal{D}_x^{\beta} u(x,t) = \simeq C^T \Lambda^2(x,1-\beta)\Lambda'(t,1)\Psi(x,t)$$
$$+\frac{x^{1-\beta}}{\Gamma(2-\beta)}(h_2(t) - h_2(0)) + {}_0^C\mathcal{D}_x^{\beta} f_0(x). \tag{34}$$

We substitute above approximations in relation (13) and collocate obtained equation in composite collocation points $(x_{n,m}, t_{n',m'})$ given in Eqs. (17) and (18). This equation gives $\hat{m}\tilde{m}$ algebraic equations; after solving this system by applying Newton's iterative scheme (Stoer and Bulirsch 2002), we achieve unknown vector C^T.

5.3 Problem c

For solving problem (c), by applying relations (22), (24) and (25), we get:

$${}_0^C\mathcal{D}_t^{\nu} u(a_2x, b_2t) \simeq {}_0^C\mathcal{D}_t^{\nu} P_{M,M'}^{k,k'} u(a_2x, b_2t) = C^T \Lambda(a_2x,\alpha)\Psi(a_2x, b_2t)$$
$$-a_2xC^T \Lambda(1,\alpha)\Psi(1, b_2t) + (1-a_2x){}_0^C\mathcal{D}_t^{\nu} g_0(b_2t) + a_2x{}_0^C\mathcal{D}_t^{\nu} g_1(b_2t), \tag{35}$$

and

$$u(a_0x, b_0t) \simeq P_{M,M'}^{k,k'} u(a_0x, b_0t) = C^T \Lambda'(b_0t,\nu)\Lambda(a_0x,\alpha)\Psi(a_0x, b_0t)$$
$$-a_0xC^T \Lambda'(b_0t,\nu)\Lambda(1,\alpha)\Psi(1, b_0t) + \omega(a_0x, b_0t), \tag{36}$$

and

$$
{}_0^C\mathcal{D}_x^{\beta}u(a_1x,b_1t) \simeq {}_0^C\mathcal{D}_x^{\beta}P_{M,M'}^{k,k'}u(a_1x,b_1t) = C^T\Lambda'(b_1t,\nu)\Lambda(a_1x,\alpha-\beta)\Psi(a_1x,b_1t) - \frac{(a_1x)^{1-\beta}}{\Gamma(2-\beta)}C^T\Lambda'(b_1t,\nu)\Lambda(1,\alpha)\Psi(1,b_1t) + {}_0^C\mathcal{D}_x^{\beta}\omega(a_1x,b_1t). \tag{37}
$$

By substituting Eqs. (20) and (35)–(37) into Eq. (16) and taking composite collocation points $(x_{n,m}, t_{n',m'}, n = 1, 2, \ldots, 2^{k-1}, m = 0, 1, \ldots, M-1, n' = 1, 2, \ldots, 2^{k'-1}, m' = 0, 1, \ldots, M'-1)$, in the obtained equation, we get:

$$
{}_0^C\mathcal{D}_x^{\alpha}P_{M,M'}^{k,k'}u\left(x_{n,m},t_{n',m'}\right) = F\Big(x_{n,m}, t_{n,m}, P_{M,M'}^{k,k'}u\left(a_0x_{n,m},b_0t_{n',m'}\right), {}_0^C\mathcal{D}_x^{\beta}P_{M,M'}^{k,k'}u\left(a_1x_{n,m},b_1t_{n',m'}\right), {}_0^C\mathcal{D}_t^{\nu}P_{M,M'}^{k,k'}u\left(a_2x_{n,m},b_2t_{n',m'}\right)\Big). \tag{38}
$$

This system is solved using Newton iteration scheme (Stoer and Bulirsch 2002) for finding vector C. Therefore, we achieve the approximate solution of the problem (c).

6 Convergence analysis

In this part, we derive the convergence of the approximate solution with respect to the bivariate Müntz–Legendre wavelets basis. Then, we give an error analysis of present method.

6.1 Error bound for the interpolation

We indicate convergence the bivariate MLWs expansion of a function $u(x,t)$. First, we present some necessary symbols as:

$$
\begin{aligned}
&I_{k,n} = \left[\frac{n-1}{2^{k-1}}, \frac{n}{2^{k-1}}\right), \quad I_{k',n'} = \left[\frac{n'-1}{2^{k'-1}}, \frac{n'}{2^{k'-1}}\right),\\
&\Lambda = I_{k,n}\times I_{k',n'}, \quad \Omega = [0,1)\times[0,1),\\
&R_{M,M'}^{k,k'} = \sup\nolimits_{(x,t)\in\Omega}\left|{}_0^C\mathcal{D}_x^{M\gamma}\left({}_0^C\mathcal{D}_t^{M'\gamma}u(x,t)\right)\right|,\\
&r_{M,M'}^{k,k'} = \sup\nolimits_{(x,t)\in\Lambda}\left|{}_0^C\mathcal{D}_x^{M\gamma}\left({}_0^C\mathcal{D}_t^{M'\gamma}u(x,t)\right)\right|,\\
&L^2(\Omega) = \{\vartheta : \vartheta \text{ is measurable on } \Omega \text{ and } \|\vartheta\| < \infty\}.
\end{aligned}
$$

Theorem 1 *Let ${}_0^C\mathcal{D}_x^{i\gamma}\left({}_0^C\mathcal{D}_t^{j\gamma}u(x,t)\right) \in C(\Omega)$ for $i = 0, 1, \ldots, M$; $j = 0, 1, \ldots, M'$ and $\Delta_{M,M'}^{k,k'} = span\{L_{0,1}(x,t), L_{0,2}(x,t), \ldots, L_{0,M'-1}(x,t), L_{1,0}(x,t)\ldots, L_{M-1,M'-1}(x,t)\}$. If we show the best approximation solution of function $u(x,t)$ from $\Delta_{M,M'}^{k,k'}$ on Λ by $p_{M,M'}^{k,k'}u(x,t)$, then the error bound of the approximate solution $P_{M,M'}^{k,k'}u(x,t)$ by applying bivariate Müntz–Legendre wavelets series on the interval Ω would be obtained as:*

$$
\|u(x,t) - P_{M,M'}^{k,k'}u(x,t)\|_{L^2(\Omega)} \le \frac{R_{M,M'}^{k,k'}}{\Gamma(M\gamma+1)\Gamma(M'\gamma+1)\sqrt{(2M\gamma+1)(2M'\gamma+1)}}. \tag{39}
$$

Proof We define:

$$h^{k,k'}_{M,M'}(x,t)=\sum_{i=0}^{M-1}\sum_{j=0}^{M'-1}\frac{x^{i\gamma}t^{j\gamma}}{\Gamma(i\gamma+1)\Gamma(j\gamma+1)}{}_0^C\mathcal{D}_x^{i\gamma}\left({}_0^C\mathcal{D}_t^{j\gamma}u(x,t)\right)\Big|_{(0,0)}. \quad (40)$$

Multi-variable Taylor formula (Hormander 1990) and generalized Taylor's formula (Odibat and Shawagfeh 2007) yield:

$$|u(x,t)-h^{k,k'}_{M,M'}(x,t)|\leq\frac{x^{M\gamma}t^{M'\gamma}}{\Gamma(M\gamma+1)\Gamma(M'\gamma+1)}r^{k,k'}_{M,M'}. \quad (41)$$

Since $p^{k,k'}_{M,M'}u(x,t)$ is the best approximation solution of $u(x,t)$ out of $\Delta^{k,k'}_{M,M'}$ on Λ, we get:

$$\begin{aligned}\|u(x,t)-P^{k,k'}_{M,M'}u(x,t)\|^2_{L^2(\Omega)}&=\|u(x,t)-C^T\Psi(x,t)\|^2_{L^2(\Omega)}\\&=\sum_{n=1}^{2^{k-1}}\sum_{n'=1}^{2^{k'-1}}\|u(x,t)-p^{k,k'}_{M,M'}u(x,t)\|^2_{L^2(\Lambda)}\\&\leq\sum_{n=1}^{2^{k-1}}\sum_{n'=1}^{2^{k'-1}}\|u(x,t)-h^{k,k'}_{M,M'}(x,t)\|^2_{L^2(\Lambda)}\\&\leq\sum_{n=1}^{2^{k-1}}\sum_{n'=1}^{2^{k'-1}}\int_{I_{k,n}}\int_{I_{k',n'}}\left[\frac{x^{M\gamma}t^{M'\gamma}}{\Gamma(M\gamma+1)\Gamma(M'\gamma+1)}r^{k,k'}_{M,M'}\right]^2\mathrm{d}t\mathrm{d}x\\&\leq\int_0^1\int_0^1\left[\frac{x^{M\gamma}t^{M'\gamma}}{\Gamma(M\gamma+1)\Gamma(M'\gamma+1)}R^{k,k'}_{M,M'}\right]^2\mathrm{d}t\mathrm{d}x\\&\leq\frac{1}{\Gamma(M\gamma+1)^2\Gamma(M'\gamma+1)^2(2M\gamma+1)(2M'\gamma+1)}(R^{k,k'}_{M,M'})^2,\end{aligned} \quad (42)$$

as a result of Eq. (42), we get Eq. (39) □

Now, we can express the convergence of the presented scheme, which depends on two parameters (M, M'). By increasing M, M', it implies that:

$$M,M'\to\infty,\quad \|u(x,t)-P^{k,k'}_{M,M'}u(x,t)\|_{L^2(\Omega)}\to 0.$$

6.2 Error analysis of present method

Now, we want to obtain error of present method; for this aim, we present following theorems.

Theorem 2 *Suppose that $u(x,t)$, $p^{k,k'}_{M,M'}u(x,t)$ and ${}_0^C\mathcal{D}_x^{i\gamma}({}_0^C\mathcal{D}_t^{j\gamma}u(x,t))$ satisfy the conditions of Theorem 1. Then:*

$$\begin{aligned}&\|{}_0^C\mathcal{D}_x^{\alpha}u(x,t)-{}_0^C\mathcal{D}_x^{\alpha}P^{k,k'}_{M,M'}u(x,t)\|_{L^2(\Omega)}\\&\leq\frac{1}{\Gamma(M\gamma+1-\alpha)\Gamma(M'\gamma+1)\sqrt{(2M\gamma-2\alpha+1)(2M'\gamma+1)}}R^{k,k'}_{M,M'}.\end{aligned} \quad (43)$$

Proof According to Eq. (40) and properties of Caputo fractional derivative, we can write:

$$\left|{}_0^C\mathcal{D}_x^{\alpha}u(x,t)-{}_0^C\mathcal{D}_x^{\alpha}h_{M,M'}^{k,k'}(x,t)\right|\leq\frac{x^{M\gamma-\alpha}t^{M'\gamma}}{\Gamma(M\gamma+1-\alpha)\Gamma(M'\gamma+1)}r_{M,M'}^{k,k'};\tag{44}$$

then:

$$\begin{aligned}&\left\|{}_0^C\mathcal{D}_x^{\alpha}u(x,t)-{}_0^C\mathcal{D}_x^{\alpha}P_{M,M'}^{k,k'}u(x,t)\right\|_{L^2(\Omega)}^2\\&=\sum_{n=1}^{2^{k-1}}\sum_{n'=1}^{2^{k'-1}}\left\|{}_0^C\mathcal{D}_x^{\alpha}u(x,t)-{}_0^C\mathcal{D}_x^{\alpha}p_{M,M'}^{k,k'}u(x,t)\right\|_{L^2(\Lambda)}^2\\&\leq\sum_{n=1}^{2^{k-1}}\sum_{n'=1}^{2^{k'-1}}\left\|{}_0^C\mathcal{D}_x^{\alpha}u(x,t)-{}_0^C\mathcal{D}_x^{\alpha}h_{M,M'}^{k,k'}(x,t)\right\|_{L^2(\Lambda)}^2\\&\leq\sum_{n=1}^{2^{k-1}}\sum_{n'=1}^{2^{k'-1}}\int_{I_{k,n}}\int_{I_{k',n'}}\left[\frac{x^{M\gamma-\alpha}t^{M'\gamma}}{\Gamma(M\gamma+1-\alpha)\Gamma(M'\gamma+1)}r_{M,M'}^{k,k'}\right]^2\mathrm{d}t\mathrm{d}x\\&\leq\int_0^1\int_0^1\left[\frac{x^{M\gamma-\alpha}t^{M'\gamma}}{\Gamma(M\gamma+1-\alpha)\Gamma(M'\gamma+1)}R_{M,M'}^{k,k'}\right]^2\mathrm{d}t\mathrm{d}x\\&\leq\frac{1}{\Gamma(M\gamma+1-\alpha)^2\Gamma(M'\gamma+1)^2(2M\gamma-2\alpha+1)(2M'\gamma+1)}(R_{M,M'}^{k,k'})^2.\end{aligned}\tag{45}$$

Therefore, the theorem is proved. □

Corollary 1 *According to the assumptions of Theorem 2, it yields:*

$$\begin{aligned}&\left\|{}_0^C\mathcal{D}_x^{\beta}u(x,t)-{}_0^C\mathcal{D}_x^{\beta}P_{M,M'}^{k,k'}u(x,t)\right\|_{L^2(\Omega)}\\&\leq\frac{1}{\Gamma(M\gamma+1-\beta)\Gamma(M'\gamma+1)\sqrt{(2M\gamma-2\beta+1)(2M'\gamma+1)}}R_{M,M'}^{k,k'}.\end{aligned}\tag{46}$$

Proof It is an immediate consequence of Theorem 2. □

Corollary 2 *According to the assumptions of Theorem 2, we have:*

$$\begin{aligned}&\left\|{}_0^C\mathcal{D}_t^{\nu}u(x,t)-{}_0^C\mathcal{D}_t^{\nu}P_{M,M'}^{k,k'}u(x,t)\right\|_{L^2(\Omega)}\\&\leq\frac{1}{\Gamma(M\gamma+1)\Gamma(M'\gamma+1-\nu)\sqrt{(2M\gamma+1)(2M'\gamma+1-2\nu)}}R_{M,M'}^{k,k'}.\end{aligned}\tag{47}$$

Proof It is an immediate consequence of Theorem 2. □

Theorem 3 *According to the assumptions of Theorem 2 and suppose F in Eq. (13) is Lipschitz, with the Lipschitz constants η_1, η_2 and η_3. The error bound $(E_{M,M'}^{k,k'})$ is given by:*

$$\begin{aligned}\|E_{M,M'}^{k,k'}(x,t)\|_{L^2(\Omega)}\leq&\frac{R_{M,M'}^{k,k'}}{\Gamma(M\gamma+1-\alpha)\Gamma(M'\gamma+1)\sqrt{(2M\gamma-2\alpha+1)(2M'\gamma+1)}}\\&+\eta_1\frac{R_{M,M'}^{k,k'}}{\Gamma(M\gamma+1)\Gamma(M'\gamma+1)\sqrt{(2M\gamma+1)(2M'\gamma+1)}}\end{aligned}$$

$$+\eta_2 \frac{R_{M,M'}^{k,k'}}{\Gamma(M\gamma+1-\beta)\Gamma(M'\gamma+1)\sqrt{(2M\gamma-2\beta+1)(2M'\gamma+1)}}$$
$$+\eta_3 \frac{R_{M,M'}^{k,k'}}{\Gamma(M\gamma+1)\Gamma(M'\gamma+1-\nu)\sqrt{(2M\gamma+1)(2M'\gamma+1-2\nu)}}. \quad (48)$$

Proof We know:

$$\|E_{M,M'}^{k,k'}(x,t)\|_{L^2(\Omega)} = \Big\| {}_0^C\mathcal{D}_x^\alpha P_{M,M'}^{k,k'}u(x,t) - F(x,t,P_{M,M'}^{k,k'}u(x,t), {}_0^C\mathcal{D}_x^\beta P_{M,M'}^{k,k'}u(x,t), {}_0^C\mathcal{D}_t^\nu P_{M,M'}^{k,k'}u(x,t))\Big\|_{L^2(\Omega)}. \quad (49)$$

By applying relation (13), we obtain:

$$\|E_{M,M'}^{k,k'}(x,t)\|_{L^2(\Omega)} = \Big\| {}_0^C\mathcal{D}_x^\alpha u(x,t) - F\left(x,t,u(x,t), {}_0^C\mathcal{D}_x^\beta u(x,t), {}_0^C\mathcal{D}_t^\nu u(x,t)\right) - {}_0^C\mathcal{D}_x^\alpha P_{M,M'}^{k,k'}u(x,t) + F\left(x,t,P_{M,M'}^{k,k'}u(x,t), {}_0^C\mathcal{D}_x^\beta P_{M,M'}^{k,k'}u(x,t), {}_0^C\mathcal{D}_t^\nu P_{M,M'}^{k,k'}u(x,t)\right)\Big\|_{L^2(\Omega)}, \quad (50)$$

since F satisfies a Lipschitz condition with Lipschitz constants η_1, η_2 and η_3, we have:

$$\begin{aligned}\|E_{M,M'}^{k,k'}(x,t)\|_{L^2(\Omega)} \le & \Big\| {}_0^C\mathcal{D}_x^\alpha u(x,t) - {}_0^C\mathcal{D}_x^\alpha P_{M,M'}^{k,k'}u(x,t)\Big\|_{L^2(\Omega)} \\ & +\eta_1 \Big\| u(x,t) - P_{M,M'}^{k,k'}u(x,t)\Big\|_{L^2(\Omega)} \\ & +\eta_2 \Big\| {}_0^C\mathcal{D}_x^\beta u(x,t) - {}_0^C\mathcal{D}_x^\beta P_{M,M'}^{k,k'}u(x,t)\Big\|_{L^2(\Omega)} \\ & +\eta_3 \Big\| {}_0^C\mathcal{D}_t^\nu u(x,t) - {}_0^C\mathcal{D}_t^\nu P_{M,M'}^{k,k'}u(x,t)\Big\|_{L^2(\Omega)}. \end{aligned} \quad (51)$$

Using Eqs. (39), (43), (46), and (47), we yield:

$$\begin{aligned}&\|E_{M,M'}^{k,k'}(x,t)\|_{L^2(\Omega)} \\ &\le \frac{1}{\Gamma(M\gamma+1-\alpha)\Gamma(M'\gamma+1)\sqrt{(2M\gamma-2\alpha+1)(2M'\gamma+1)}} R_{M,M'}^{k,k'} \\ &+\eta_1 \frac{1}{\Gamma(M\gamma+1)\Gamma(M'\gamma+1)\sqrt{(2M\gamma+1)(2M'\gamma+1)}} R_{M,M'}^{k,k'} \\ &+\eta_2 \frac{1}{\Gamma(M\gamma+1-\beta)\Gamma(M'\gamma+1)\sqrt{(2M\gamma-2\beta+1)(2M'\gamma+1)}} R_{M,M'}^{k,k'} \\ &+\eta_3 \frac{1}{\Gamma(M\gamma+1)\Gamma(M'\gamma+1-\nu)\sqrt{(2M\gamma+1)(2M'\gamma+1-2\nu)}} R_{M,M'}^{k,k'}; \end{aligned} \quad (52)$$

therefore, the proof is complete. □

Remark 2 Error of method of problems (b) and (c) is similar of problem (a) that we obtain above theorems.

7 Numerical experiments

In this part, we present five examples to show the validity and applicability of the applied technique. The computations were performed on a personal computer, and the codes were written in Mathematica 10.

7.1 Problem a

Example 1 Consider the space-time-fractional Convection–Diffusion equation as: (Wei et al. 2012; Chen et al. 2014)

$$
{}_0^C\mathcal{D}_t^{\nu} u(x,t) + x^{0.8} u_x(x,t) - (\Gamma(2.8)x/2)\,{}_0^C\mathcal{D}_x^{\alpha} u(x,t) + x^{1.5} u(x,t) = f(x,t), \quad 0 \le x, t < 1, \tag{53}
$$

where

$$
f(x,t) = \frac{\Gamma(3)x^2(1-x)t^{1.2}}{\Gamma(2.2)} + \left[2x^{1.8} - 3x^{2.8} - \frac{\Gamma(2.8)\Gamma(3)x^{1.5}}{2\Gamma(1.5)} + \frac{\Gamma(2.8)\Gamma(4)x^{2.5}}{2\Gamma(2.5)} + x^{3.5} - x^{4.5}\right] t^2
$$

and

$$
u(x,0) = u(0,t) = u(1,t) = 0.
$$

For the above equation, we have the analytical solution $u(x,t) = x^2(1-x)t^2$, when $\alpha = 1.5$, $\nu = 0.8$.

In Tables 1 and 2 we compare absolute error of proposed scheme for $M = M' = 3$; $k = k' = 2$; $\gamma = 1$ with Haar wavelet method (Chen et al. 2014) for $m = n = 3$ and Tau method based on fractional-order Legendre functions (Wei et al. 2012) for $m = 8$. Also, CPU time of suggested scheme is presented in Tables 1 and 2.

Example 2 Consider the following nonlinear fractional heat equation as: Daftardar-Gejji and Bhalekar (2010)

$$
{}_0^C\mathcal{D}_t^{\nu} u(x,t) = u_{xx}(x,t) + u(x,t)u_x(x,t), \quad 0 < \nu \le 1, \tag{54}
$$

subject to

$$
u(x,0) = 2 - x, \quad u(0,t) = \frac{2}{1+t}, \quad u(1,t) = \frac{1}{1+t}.
$$

Table 1 Comparison of absolute error for $k = k' = 2$, $\gamma = 1$ of Example 1

(x,t)	Chen et al. (2014) $m = n = 3$	Our method $M = M' = 3$
(0.1, 0.1)	2.09×10^{-4}	1.30×10^{-5}
(0.4, 0.1)	1.62×10^{-3}	9.78×10^{-5}
(0.7, 0.1)	2.20×10^{-3}	4.82×10^{-6}
(0.1, 0.5)	3.24×10^{-3}	7.54×10^{-3}
(0.7, 0.5)	9.34×10^{-3}	1.63×10^{-6}
CPU times	–	1.25

Table 2 Comparison of absolute error for $k = k' = 2, \gamma = 1$ of Example 1

(x, t)	Wei et al. (2012) $m = 8$	Our method $M = M' = 3$
(0, 0)	1.36×10^{-5}	0
(1/8, 1/8)	2.25×10^{-5}	1.63×10^{-5}
(2/8, 2/8)	1.45×10^{-4}	6.34×10^{-7}
(3/8, 3/8)	2.33×10^{-4}	2.76×10^{-3}
(4/8, 4/8)	2.61×10^{-4}	1.83×10^{-4}
(5/8, 5/8)	3.34×10^{-4}	4.64×10^{-4}
CPU times	–	1.25

The analytical solution is $u(x, t) = \frac{2-x}{1+t}$, when $\nu = 1$.

We solve the above problem by applying the bivariate MLWs with $M = M' = 1; k = k' = 2; \nu = 1$ and every value of γ. Let:

$$\frac{\partial^{2+\nu} u(x, t)}{\partial x^2 \partial t^\nu} \simeq c_0\psi_0(x, t) + c_1\psi_1(x, t) + c_2\psi_2(x, t) + c_3\psi_3(x, t) = C^T \Psi(x, t), \quad (55)$$

where

$$C^T = [c_0, c_1, c_2, c_3], \quad \Psi(x, t) = [\psi_0(x, t), \psi_1(x, t), \psi_2(x, t), \psi_3(x, t)]^T.$$

Using Eqs. (20), (22), (24), (25), (55), and conditions of problem for $\alpha = 2, \beta = 1$, achieve:

$$u_{xx}(x, t) \simeq C^T \Lambda'(t, \nu)\Psi(x, t), \quad (56)$$

$${}_0^C\mathcal{D}_t^\nu u(x, t) \simeq C^T \Lambda(x, 2)\Psi(x, t) - xC^T \Lambda(1, 2)\Psi(1, t) + \frac{x - 2}{(1 + t)^2}, \quad (57)$$

$$u(x, t) \simeq C^T \Lambda'(t, \nu)\Lambda(x, 2)\Psi(x, t) - xC^T \Lambda'(t, \nu)\Lambda(1, 2)\Psi(1, t) + \frac{2 - x}{1 + t}, \quad (58)$$

and

$$u_x(x, t) \simeq C^T \Lambda'(t, \nu)\Lambda(x, 1)\Psi(x, t) - C^T \Lambda'(t, \nu)\Lambda(1, 2)\Psi(1, t) - \frac{1}{1 + t}. \quad (59)$$

By substituting Eqs. (56)–(59) into Eq. (54) and collocating this equation in the following composite collocation points:

$$x_{1,0} = t_{1,0} = 0.25, \quad x_{1,1} = t_{1,1} = 0.75,$$

and by solving the obtained system of equations yields:

$$c_0 = c_1 = c_2 = c_3 = 0.$$

Therefore, by employing relation (58), we obtain $u(x, t) = \frac{2-x}{1+t}$ which is the analytical solution of problem.

In Fig. 3, we compare our numerical results with a iterative technique in Daftardar-Gejji and Bhalekar (2010), Adomian decomposition technique, and the exact solution for case $\nu = 1$ at $t = 0.3$. Figure 4a, b shows approximate solutions with Daftardar-Gejji and Bhalekar (2010) and the suggested method, respectively, for $\nu = 1$. Also, the CPU time (in seconds) of this problem is 0.250.

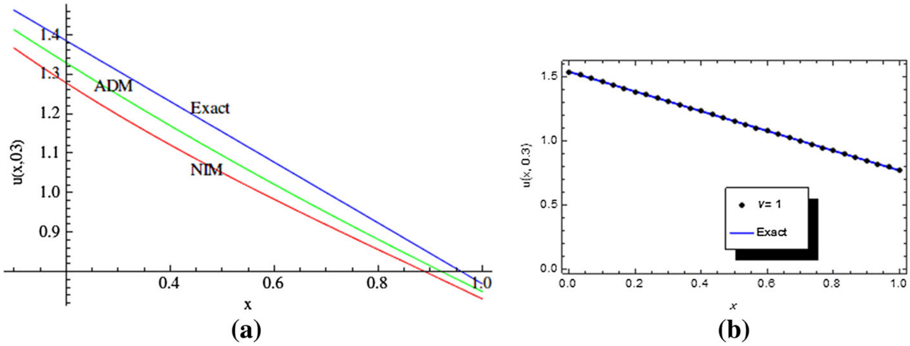

Fig. 3 Comparison of our numerical results at $M = M' = 1, k = k' = 2$ with other schemes of Example 2

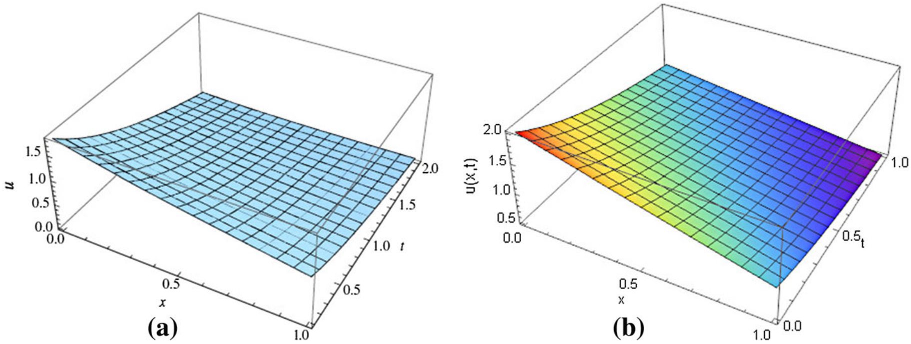

Fig. 4 Comparison of our numerical results at $M = M' = 1, k = k' = 2$ with iterative scheme of Example 2

7.2 Problem b

Example 3 Consider the space fractional advection-dispersion equation as: Momani and Odibat (2008)

$$ {}_0^C\mathcal{D}_x^{\alpha} u(x,t) = u_x(x,t) + u_t(x,t) + f(x,t), \quad 1 < \alpha \leq 2, \tag{60} $$

where

$$ f(x,t) = 2 - 2t - 2x, $$

subject to:

$$ u(x,0) = x^2, \quad u(0,t) = t^2, \quad u_x(0,t) = 0. $$

For the above equation, we have the analytical solution $u(x,t) = x^2 + t^2$ when $\alpha = 2$.

For solving the above example, we let $k = k' = 2$, $M = M' = 2$, with every value of $0 < \gamma \leq 1$. Using approximating $\frac{\partial^3 u(x,t)}{\partial x^2 \partial t}$, we obtain:

$$ \frac{\partial^3 u(x,t)}{\partial x^2 \partial t} \simeq \sum_{i=0}^{15} c_i \psi_i(x,t) = C^T \Psi(x,t). \tag{61} $$

From Eqs. (32), (30), and (31), we have:

$$ {}_0^C\mathcal{D}_x^{\alpha} u(x,t) \simeq C^T \Lambda'(t,1)\Lambda(x,2-\alpha)\Psi(x,t) + \frac{2}{\Gamma(3-\alpha)}x^{2-\alpha}, \tag{62}$$

$$\frac{\partial u(x,t)}{\partial t} \simeq C^T \Lambda^2(x,1)\Psi(x,t) + 2t, \tag{63}$$

and

$$u(x,t) \simeq C^T \Lambda^2(x,1)\Lambda'(t,1)\Psi(x,t) + x^2 + t^2. \tag{64}$$

Now, by derivative from Eq. (64) of order 1 with respect to x, achieve:

$$\frac{\partial u(x,t)}{\partial x} \simeq C^T \Lambda(x,1)\Lambda'(t,1)\Psi(x,t) + 2x. \tag{65}$$

By substituting Eqs. (62)–(65) into Eq. (60) and collocating this equation in the following composite collocation point:

$$x_{1,0} = t_{1,0} = 0.105662, \quad x_{1,1} = t_{1,1} = 0.394338,$$
$$x_{2,0} = t_{2,0} = 0.605662, \quad x_{2,1} = t_{2,1} = 0.894338,$$

and by solving the obtained system of equations yields:

$$c_i = 0, \quad i = 0, 1, \ldots, 15.$$

By applying relation (64), we obtain the exact value $u(x,t)$ for $\alpha = 2$. Also, The CPU time (in seconds) of this problem for this case is 0.625.

We plot the numerical solution of $u(0.6,t)$ and $u(x,0.6)$ for $\gamma = 1$ with different values of α in Fig. 5a, b. Results indicate that when α approaches to 2, the numerical solutions tend to the analytical solution. Figures. 6, 7, 8 represent the graphs of the numerical solutions and contour plot using the proposed method with $\gamma = \frac{1}{3}$ and $M = M' = 2; k = k' = 2$ for $\alpha = 2, 1.9, 1.8$, respectively.

Example 4 Consider the following time FPDEs as (Chen et al. 2010; Saadatmandi et al. 2012):

$$ {}_0^C\mathcal{D}_t^{\nu} u(x,t) = -u_{xx}(x,t) - x u_x(x,t) + f(x,t), \quad 0 < \nu \leq 1, \tag{66}$$

where

$$f(x,t) = 2x^2 + 2t^{\nu} + 2,$$

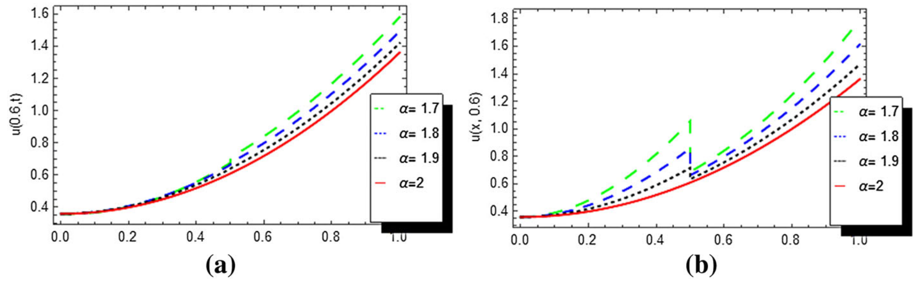

Fig. 5 Numerical solution of present approach for different values of α with $k = k' = 2$, $M = M' = 2$, $\gamma = 1$ for Example 3

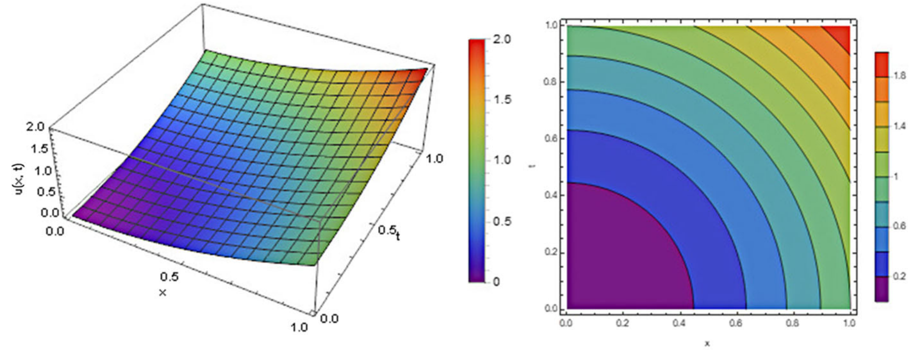

(a) **(b)**

Fig. 6 **a** Numerical solution and **b** contour plot with $\alpha = 2$ and $\gamma = \frac{1}{3}$ for Example 3

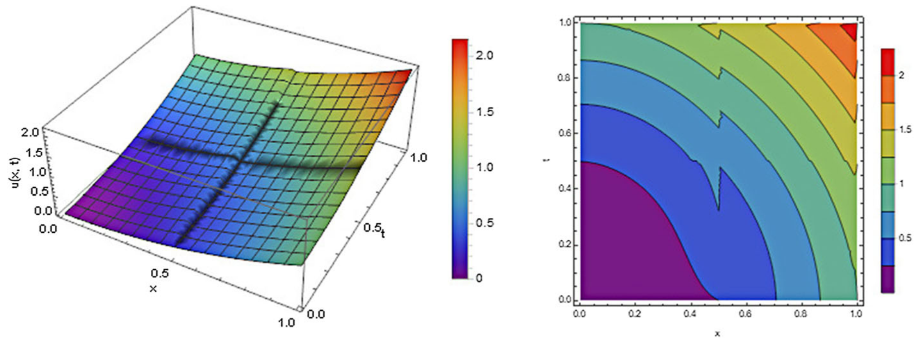

(a) **(b)**

Fig. 7 **a** Numerical solution and **b** contour plot with $\alpha = 1.9$ and $\gamma = \frac{1}{3}$ for Example 3

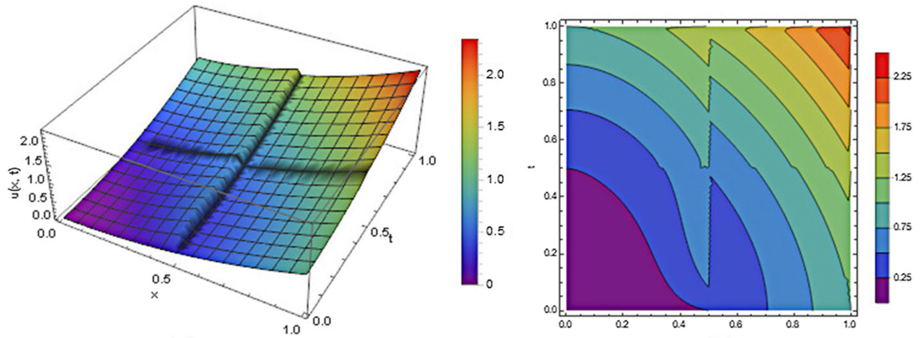

(a) **(b)**

Fig. 8 **a** Numerical solution and **b** contour plot with $\alpha = 1.8$ and $\gamma = \frac{1}{3}$ for Example 3

Table 3 Comparison of absolute error for $\nu = 0.5, t = 0.5, \gamma = \alpha$ of Example 4

x	Chen et al. (2010) $m = 64$	Saadatmandi et al. (2012) $m = 25$	Our method $k = k' = 2, M = M' = 1$
0.1	1.2×10^{-3}	6.5×10^{-6}	0
0.2	1.3×10^{-3}	1.6×10^{-5}	0
0.3	1.9×10^{-3}	2.3×10^{-5}	0
0.4	7.4×10^{-3}	2.7×10^{-5}	0
0.5	1.0×10^{-6}	2.8×10^{-5}	0
0.6	7.5×10^{-3}	2.5×10^{-5}	0
0.7	1.7×10^{-3}	2.0×10^{-5}	0
0.8	5.0×10^{-3}	1.3×10^{-5}	0
0.9	1.7×10^{-2}	4.7×10^{-6}	0
CPU times	–	–	0.016

subject to:

$$u(x,0) = x^2, \quad u(0,t) = \frac{2\Gamma(\nu+1)}{\Gamma(2\nu+1)} t^{2\nu}, \quad u_x(0,t) = 0.$$

For above equation, we have the exact solution $u(x,t) = x^2 + \frac{2\Gamma(\nu+1)}{\Gamma(2\nu+1)} t^{2\nu}$ when $\nu = 1$.

For solving the above example, we let $k = k' = 2, M = M' = 1$ with every value of $0 < \gamma, \nu \leq 1$. By attention Eqs. (33), (29), and (31), yield:

$$ {}_0^C\mathcal{D}_t^{\nu} u(x,t) \simeq C^T \Lambda^2(x,1)\Lambda'(t,1-\nu)\Psi(x,t) + 2t^{\nu}, \tag{67}$$

$$u_{xx}(x,t) \simeq C^T \Lambda'(t,1)\Psi(x,t) + 2, \tag{68}$$

and

$$u(x,t) \simeq C^T \Lambda^2(x,1)\Lambda'(t,1)\Psi(x,t) + \frac{2\Gamma(\nu+1)}{\Gamma(2\nu+1)} t^{2\nu} + x^2. \tag{69}$$

By derivative from Eq. (69) of order 1 with respect to x, we obtain:

$$u_x(x,t) \simeq C^T \Lambda(x,1)\Lambda'(t,1)\Psi(x,t) + 2x. \tag{70}$$

By substituting Eqs. (67)–(70) into Eq. (66) and collocating this equation in the composite collocation points given in (17) and (18), we obtain the unknown vector C, and by applying Eq. (69), we achieve the exact solution for every value of ν.

Table 3 establishes the comparison of absolutes error of suggested scheme for $M = M' = 1, k = k' = 2$ together with the Haar wavelet (Chen et al. 2010) for $m = 64$ and Sinc–Legendre collocation technique (Saadatmandi et al. 2012) for $m = 25$. The graphs of numerical solution and contour plot are shown in Fig. 9a, b.

7.3 Problem c

Example 5 Consider the time fractional Burgers equation with proportional delay as Singh and Kumar (2017):

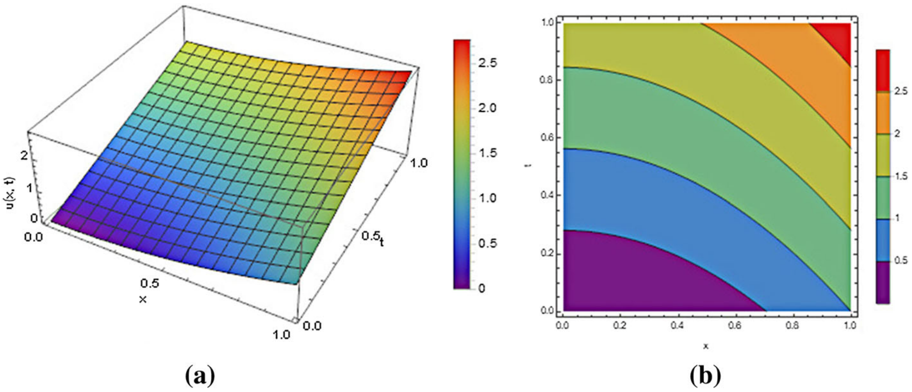

Fig. 9 **a** Numerical solution and **b** contour plot with $\gamma = \nu = 0.5$ of Example 4

$$ {}_{0}^{C}\mathcal{D}_{t}^{\nu}u(x,t) = u_{xx}(x,t) + u\left(\frac{x}{2},\frac{t}{2}\right)u_{x}\left(x,\frac{t}{2}\right) + \frac{1}{2}u(x,t), \quad 0 < \nu \leq 1, \tag{71} $$

subject to:

$$ u(x,0) = x, \quad u(0,t) = 0, \quad u(1,t) = e^{t}. $$

For above equation, we have the analytical solution $u(x,t) = xe^{t}$ when $\nu = 1$.

For numerical solution of this example, we select $k = k' = 2$; $M = M' = 2$ and $\gamma = \frac{1}{2}$. From Eqs. (20), (22), (36), (37), and (24) for $\alpha = 2$ and $\beta = 1$, we have:

$$ u_{xx}(x,t) \simeq C^{T}\Lambda'(t,\nu)\Psi(x,t), \tag{72} $$

$$ {}_{0}^{C}\mathcal{D}_{t}^{\nu}u(x,t) \simeq C^{T}\Lambda(x,2)\Psi(x,t) - xC^{T}\Lambda(1,2)\Psi(1,t) + xt^{1-\nu}E_{1,2-\nu}(t), \tag{73} $$

$$ u\left(\frac{x}{2},\frac{t}{2}\right) \simeq C^{T}\Lambda'\left(\frac{t}{2},\nu\right)\Lambda\left(\frac{x}{2},2\right)\Psi\left(\frac{x}{2},\frac{t}{2}\right) - \frac{x}{2}C^{T}\Lambda'\left(\frac{t}{2},\nu\right)\Lambda(1,2)\Psi\left(1,\frac{t}{2}\right) + \frac{x}{2}e^{\frac{t}{2}}, \tag{74} $$

$$ u_{x}\left(x,\frac{t}{2}\right) \simeq C^{T}\Lambda'\left(\frac{t}{2},\nu\right)\Lambda(x,1)\Psi\left(x,\frac{t}{2}\right) - C^{T}\Lambda'\left(\frac{t}{2},\nu\right)\Lambda(1,2)\Psi\left(1,\frac{t}{2}\right) + e^{\frac{t}{2}}, \tag{75} $$

$$ u(x,t) \simeq C^{T}\Lambda'(t,\nu)\Lambda(x,2)\Psi(x,t) - xC^{T}\Lambda'(t,\nu)\Lambda(1,2)\Psi(1,t) + xe^{t}. \tag{76} $$

By substituting Eqs. (72)–(76) into Eq. (71) and collocating this equation in the composite collocation points given in (17) and (18), and Newton's iterative scheme, we achieve the analytical solution for $\nu = 1$.

Table 4 displays the absolute error of suggested scheme by choosing $k = k' = 2$; $M = M' = 2$; $\nu = 1$ and $\gamma = \frac{1}{2}, 1$ together with homotopy perturbation transform method (Singh and Kumar 2017). In addition, CPU time for $\gamma = \frac{1}{2}$ and $\gamma = 1$ are revealed in Table 4. The plots of the solution with present method and Singh and Kumar (2017) for various values of $\nu = 0.8, 0.9, 1$ are depicted in Fig. 10. Also, the numerical solutions behavior of $u(x,t)$ and contour plots for various values of $\nu = 0.8, 0.9, 1$ are depicted in Figs. 11, 12, and 13.

Table 4 Comparison of absolute error for $k = k' = 2$, $M = M' = 2$, $\gamma = \frac{1}{2}, 1$ for Example 5

x	t	Singh and Kumar (2017)	Our method	
			$\gamma = \frac{1}{2}$	$\gamma = 1$
0.25	0.25	2.122401×10^{-6}	0	0
	0.50	7.094268×10^{-5}	0	0
	0.75	5.634807×10^{-4}	0	0
	1.00	2.487124×10^{-3}	0	0
0.5	0.25	4.244802×10^{-6}	0	0
	0.50	1.418854×10^{-4}	0	0
	0.75	1.126961×10^{-3}	0	0
	1.00	4.974248×10^{-3}	0	0
0.75	0.25	6.369688×10^{-6}	0	0
	0.50	2.128250×10^{-4}	0	0
	0.75	1.690020×10^{-3}	0	0
	1.00	7.461370×10^{-3}	0	0
CPU times		–	2.593	0.250

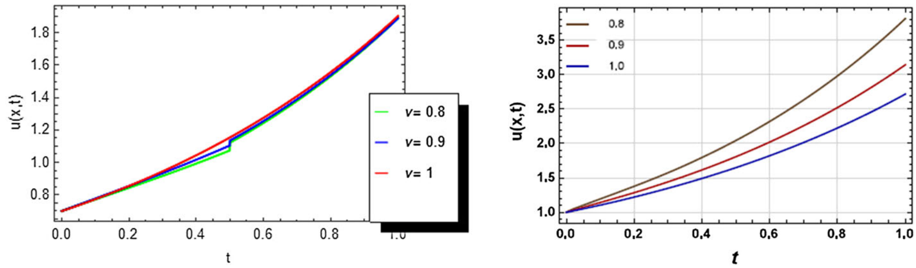

Fig. 10 Approximate solutions of (left side): present method with $\gamma = 1$ and (right side): Singh and Kumar (2017) with $\nu = 0.8, 0.9, 1$ for Example 5

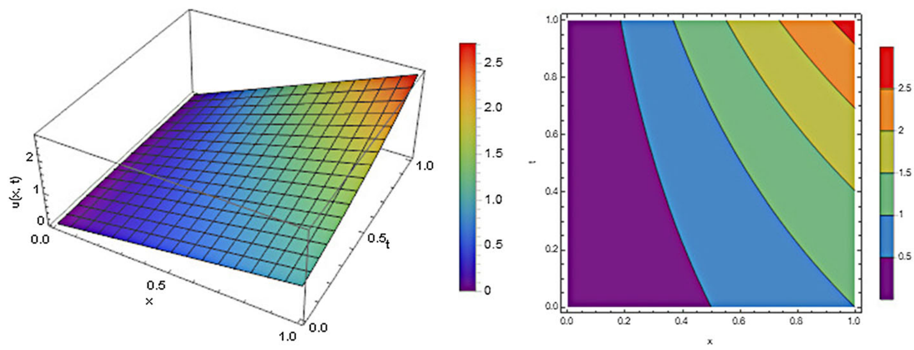

(a) **(b)**

Fig. 11 **a** Numerical solution and **b** contour plot with $\nu = 1$, $\gamma = \frac{1}{2}$ for $M = M' = 2$ and $k = k' = 2$ of Example 5

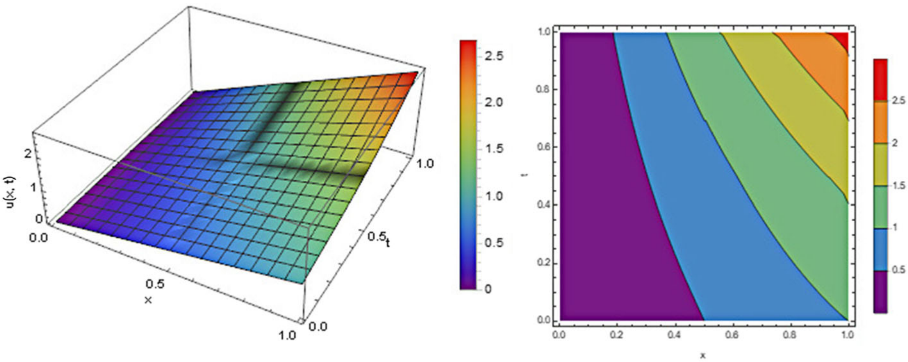

(a) **(b)**

Fig. 12 **a** Numerical solution and **b** contour plot with $\nu = 0.9, \gamma = \frac{1}{2}$ at $M = M' = 2$ and $k = k' = 2$ of Example 5

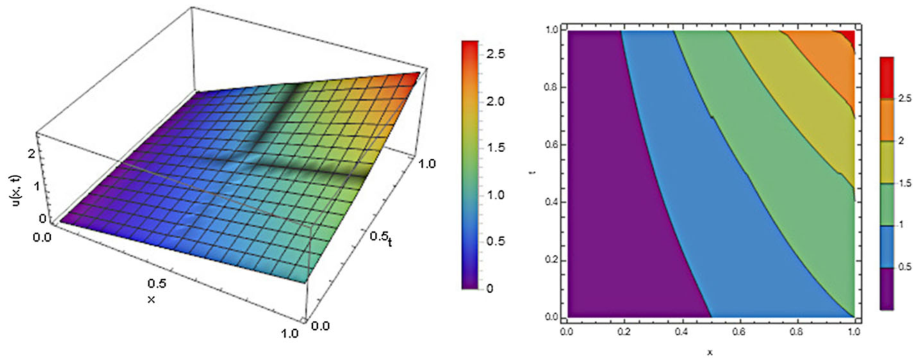

(a) **(b)**

Fig. 13 **a** Numerical solution and **b** contour plot with $\nu = 0.8, \gamma = \frac{1}{2}$ for $M = M' = 2$ and $k = k' = 2$ of Example 5

8 Discussion and future work

The aim of this study was to present an effective numerical algorithm for solving three classes of FPDEs using bivariate MLWs. The MLWs' operational matrix of fractional integration is derived. This operational matrix and the composite collocation scheme are used to transform FPDEs into systems of nonlinear equations to provide an approximate solution of FPDEs. The obtained results by our technique emphasized that:

1. The scheme is very easy to implement and achieves high accurate approximate solutions.
2. Few terms of bivariate MLWs are applied to provide effective and accuracy results.
3. The bivariate MLWs' scheme has less CPU time when compared to the other schemes.
4. There are three degrees of freedom (k, M, γ) for MLWs, but two degrees of freedom (k, M) for other wavelets.
5. Stability analysis of the suggested technique for numerical solution of FPDEs is an interesting problem for future work.

Acknowledgements The second author is supported by the Alzahra university within project 97/1/216. Also, we express our sincere thanks to the anonymous referees for valuable suggestions that improved the paper.

References

Abd-Elhameed WM, Youssri YH (2018) Fifth-kind orthonormal Chebyshev polynomial solutions for fractional differential equations. Comput Appl Math 37(3):2897–2921

Abdulaziz O, Hashim I, Momani S (2008) Solving systems of fractional differential equations by homotopy-perturbation method. Phys Lett A 372:451–459

Baillie RT (1996) Long memory processes and fractional integration in econometrics. J Econom 73:5–59

Benson DA, Meerschaert MM, Revielle J (2013) Fractional calculus in hydrologic modeling: a numerical perspective. Adv Water Resour 51:479–497

Beylkin G, Coifman R, Rokhlin V (1991) Fast wavelet transforms and numerical algorithms I. Commun Pure Appl Math 44:141–183

Bhrawy AH, Baleanu D (2013) A spectral Legendre–Gauss–Lobatto collocation method for a spacefractional advection–diffusion equations with variable coefficients. Rep Math Phys 72:219–233

Bhrawy AH, Zaky MA (2015) A method based on the Jacobi tau approximation for solving multi-term time-space fractional partial differential equations. J Comput Phys 281:876–895

Bohannan GW (2008) Analog fractional order controller in temperature and motor control applications. J Vib Control 14:1487–1498

Chen Y, Wu Y, Cui Y, Wang Z, Jin D (2010) Wavelet method for a class of fractional convection–diffusion equation with variable coefficients. J Comput Sci 1:146–149

Chen Y, Sun Y, Liu L (2014) Numerical solution of fractional partial differential equations with variable coefficients using generalized fractional-order Legendre functions. Appl Math Comput 244:847–858

Chui CK (1997) Wavelets: a mathematical tool for signal analysis. SIAM, Philadelphia

Daftardar-Gejji V, Bhalekar S (2010) Solving fractional boundary value problems with Dirichlet boundary conditions using a new iterative method. Comput Math Appl 59:1801–1809

Dehghan M, Abbaszadeh M (2018) A finite difference/finite element technique with error estimate for space fractional tempered diffusion-wave equation. Comput Math Appl 75(8):2903–2914

Dehghan M, Abbaszadeh M (2018) An eficient technique based on finite difference/finite element method for solution of twodimensional space/multi-time fractional Bloch-Torrey equations. Appl Numer Math 131:190–206

Dehghan M, Abbaszadeh M (2019) Error estimate of finite element/finite difference technique for solution of two-dimensional weakly singular integro-partial differential equation with space and time. J Comput Appl Math 356:314–328

Dehghan M, Safarpoor M (2016) The dual reciprocity boundary elements method for the linear and nonlinear two-dimensional time-fractional partial differential equations. Math Methods Appl Sci 39:3979–3995

Dehghan M, Manafian J, Abbaszadeh M (2010) Solving nonlinear fractional partial differential equations using the homotopy analysis method. Numer Methods Partial Differ Equ 26(2):448–479

Dehghan M, Abbaszadeh M, Mohebbi A (2016) Legendre spectral element method for solving time fractional modified anomalous sub-diffusion equation. Appl Math Model 40(5–6):3635–3654

Esmaeili sh, Shamsi M, Luchko Y (2011) Numerical solution of fractional differential equations with a collocation method based on Müntz polynomials. Comput Math Appl 62:918–929

Hall MG, Barrick TR (2008) From diffusion-weighted MRI to anomalous diffusion imaging. Magn Reson Med 59:447–455

He J (1998) Approximate analytical solution for seepage flow with fractional derivatives in porous media. Comput Methods Appl Mech Eng 167:57–68

He JH (1999) Some applications of nonlinear fractional differential equations and their approximations. Bull Sci Technol 15(2):86–90

Heydari MH, Hooshmandasl MR, Maalek Ghaini FM, Fereidouni F (2013) Two-dimensional Legendre wavelets for solving fractional Poisson equation with Dirichlet boundary conditions. Eng Anal Bound Elem 37:1331–1338

Heydari MH, Hooshmandasl MR, Mohammadi F (2014) Legendre wavelets method for solving fractional partial differential equations with Dirichlet boundary conditions. Appl Math Comput 234:267–276

Hormander L (1990) The analysis of linear partial differential operators. Springer, Berlin

Hu X, Zhang L (2012) Implicit compact difference schemes for the fractional cable equation. Appl Math Model 36:4027–4043

Lakestani M, Razzaghi M, Dehghan M (2006) Semi orthogonal spline wavelets approximation for Fredholm integro-differential equations. Math Probl Eng 2006:1–12

Lakestani M, Dehghan M, Irandoust-pakchin S (2012) The construction of operational matrix of fractional derivatives using B-spline functions. Commun Nonlinear Sci Numer Simul 17(3):1149–1162

Larsson S, Racheva M, Saedpanah F (2015) Discontinuous Galerkin method for an integro-differential equation modeling dynamic fractional order viscoelasticity. Comput Methods Appl Mech Eng 283:196–209

Li Y (2010) Solving a nonlinear fractional differential equation using Chebyshev wavelets. Commun Nonlinear Sci Numer Simul 15(9):2284–2292

Lin Y, Xu C (2007) Finite difference/spectral approximations for the time-fractional diffusion equation. J Comput Phys 225:1533–1552

Lin Y, Li X, Xu C (2011) Finite difference/spectral approximations for the fractional cable equation. Math Comput 80:1369–1396

Magin RL (2004) Fractional calculus in bioengineering. Crit Rev Biomed Eng 32:1–104

Mashayekhi S, Razzaghi M (2015) Numerical solution of nonlinear fractional integro-differential equations by hybrid functions. Eng Anal Bound Elem 56:81–89

Momani S, Odibat Z (2008) Numerical solutions of the space-time fractional advection–dispersion equation. Numer Methods Partial Differ Equ 24(6):1416–1429

Odibat Z, Shawagfeh NT (2007) Generalized Taylor's formula. Appl Math Comput 186(1):286–293

Rahimkhani P, Ordokhani Y, Babolian E (2016) Fractional-order Bernoulli wavelets and their applications. Appl Math Model 40:8087–8107

Rahimkhani P, Ordokhani Y, Babolian E (2017) Fractional-order Bernoulli functions and their applications in solving fractional Fredholem–Volterra integro-differential equations. Appl Numer Math 122:66–81

Rahimkhani P, Ordokhani Y, Babolian E (2017) A new operational matrix based on Bernoulli wavelets for solving fractional delay differential equations. Numer Algorithms 74:223–245

Rahimkhani P, Ordokhani Y, Babolian E (2018) Müntz–Legendre wavelet operational matrix of fractional-order integration and its applications for solving the fractional pantograph differential equations. Numer Algorithms 77(4):1283–1305

Rehman M, Rahmat RA (2011) The Legendre wavelet method for solving fractional differential equations. Commun Nonlinear Sci Numer Simul 16(11):4163–4173

Rossikhin YA, Shitikova MV (1997) Applications of fractional calculus to dynamic problems of linear and nonlinear hereditary mechanics of solids. Appl Mech Rev 50(1):15–67

Saadatmandi A, Dehghan M, Azizi MR (2012) The Sinc–Legendre collocation method for aclass of fractional convection–diffusion equations with variable coefficients. Commun Nonlinear Sci Numer Simul 17:4125–4136

Sabermahani S, Ordokhani Y, Yousefi SA (2018) Numerical approach based on fractional-order Lagrange polynomials for solving a class of fractional differential equations. Comput Appl Math 37(3):3846–3868

Saeedi H, Mohseni Moghadam M, Mollahasani N, Chuev GN (2011) A CAS wavelet method for solving nonlinear Fredholm integro-differential equations of fractional order. Commun Nonlinear Sci Numer Simul 16(3):1154–1163

Shamsi M, Razzaghi M (2005) Solution of Hallen's integral equation using multiwavelets. Comput Phys Commun 168:187–197

Singh BK, Kumar P (2017) Homotopy perturbation transform method for solving fractional partial differential equations with proportional delay. SeMA 75(1):111–125

Stoer J, Bulirsch R (2002) Introduction to numerical analysis, 2nd edn. Springer, Berlin

Wei J, Chen Y, Li B, Yi M (2012) Numerical solution of space-time fractional convection–diffusion equations with variable coefficients using Haar wavelets. Comput Model Eng Sci 89(6):481–495

Zheng M, Liu F, Turner I, Anh V (2015) A novel high order space-time spectral method for the time fractional Fokker–Planck equation. SIAM J Sci Comput 37:A701–A724

Zhu L, Fan Q (2013) Numerical solution of nonlinear fractionalorder Volterra integro-differential equations by SCW. Commun Nonlinear Sci Numer Simul 18(5):1203–1213